The Effect of Pore Structure on Fluid-Solid Reactions: Application to the SO_2-Lime Reaction

S. K. BHATIA
and
D. D. PERLMUTTER

Department of Chemical Engineering
University of Pennsylvania
Philadelphia, Pennsylvania 19104

The effect of varying pore structures on the kinetics of fluid-solid reactions is investigated through the random pore model developed in prior papers (Bhatia and Perlmutter, 1980, 1981). By considering several idealized pore-size distributions it is shown that a solid having a uniform pore size is intrinsically less reactive than one possessing a pore-size distribution. For solids with bimodal pore size distributions optimal structures are shown to exist for which the reactivity is a maximum.

Numerical solutions were obtained to the model equations for various values of the parameters characterizing the pore structure, the diffusion, and the chemical kinetics. The results show that the conversion-time behavior and the expected ultimate conversion can be very sensitive to variations in surface area and porosity for reactions accompanied by an increase in volume of the solid phase.

These findings are in agreement with experimental literature on the SO_2-lime reaction (Ulerich et al., 1978; Borgwardt and Harvey, 1972; Potter, 1969; Falkenberry and Slack, 1968) and the model is shown to fit the data of Borgwardt (1970), and of Hartman and Coughlin (1974, 1976). It is seen that this reaction is diffusion controlled under the conditions of Hartman and Coughlin, in consonance with their own finding using the grain model, and a prior Pigford and Sliger (1973) interpretation. The temperature behavior of the diffusion coefficient in the product layer suggests the participation of an activated process, possibly a solid state diffusion step.

SCOPE

Results are reported on the effects of pore structure differences on the reaction behavior of solids, particularly in terms of variations in surface area, porosity, and dispersion in the pore size distribution. The analysis utilizes the random pore model developed by Bhatia and Perlmutter (1980, 1981), representing a further development of these prior treatments.

To demonstrate its use the model is applied to the data of Borgwardt (1970) and Hartman and Coughlin (1974, 1976) on the lime-SO_2 reaction. The evaluation includes examination of the relative diffusional and kinetic resistances, of the incomplete conversions arising from pore closure in the solid, and of optimal pore distributions. Further comparisons are made with experimental reports of Ulerich et al. (1978), Borgwardt (1970), and Falkenberry and Slack (1968), to relate pore-structure to the frequently observed differences in reaction behavior.

CONCLUSIONS AND SIGNIFICANCE

An analysis of various simple pore size distributions shows that of all the pore structures with the same surface area and porosity, the one with pores of uniform size offers the least intrinsic reactivity. For bimodal pore size distributions optimal structures exist for which the reactivity is a maximum. Such results may offer guidance in the compaction of microporous solids by suggesting the desired pore structure.

As expected, reactivity generally increases with surface area, but such variation can reduce ultimate conversion by more rapidly plugging pores at the particle surface. Practical design thus calls for a tradeoff between reduced residence times and improved overall conversions in choosing the proper surface area of the reactant solid. The same is also found to be the case with the pore dispersion parameter ψ of the model, although its effect is found to be weak when the product layer diffusional resistance is high. Increase in porosity increases reactivity as well as ultimate conversion.

Application of the model to the data of Hartman and Coughlin (1974, 1976) on the SO_2-lime reaction shows their system to be controlled by diffusional resistances alone, and to be independent of the kinetic rate constant over the range of values reported by previous investigators (Ramachandran and Smith, 1977; Hartman and Coughlin, 1976; Wen and Ishida, 1973). The data of Borgwardt (1970) for the same reaction is however explained by a combination of kinetic and diffusional resistances. The temperature behavior of the product layer diffusivity estimated from the data of Borgwardt suggests the possibility of an activated solid state diffusional step.

S. K. Bhatia is with Mobil Research & Development Corp., Paulsboro, NJ 08066.

0001-1541-81-4375-0226-$2.00. © The American Institute of Chemical Engineers, 1981.

INTRODUCTION

In prior work on fluid-solid chemical reactions (Bhatia and Perlmutter, 1980, 1981) a model was developed for reactions of the type:

$$aA(g) + bB(s) \rightarrow pP(g) + qQ(s) \tag{1}$$

in terms of the growth and intersection of reaction surfaces within a solid particle. In contrast to the earlier grain models (Szekely et al., 1976), which utilize information on grain size distribution, the new model utilizes the pore structure characteristics of the solid. It was shown that in the presence of a significant product layer resistance to the diffusion of reactant A, the local rate of conversion at any position within the particle of solid B may be expressed as

$$\frac{dX}{d\tau} = \frac{C^*(1-X)\sqrt{1-\psi ln(1-X)}}{1+\frac{\beta Z}{\psi}\left[\sqrt{1-\psi ln(1-X)}-1\right]} \tag{2}$$

where the pore structure characteristics required by the model are the porosity, surface area, and total pore length, contained within the definitions of ψ, β, and τ. The model combined Eq. 2 for reaction rate with the common conservation and diffusional laws for spherical geometry with no bulk flow:

$$\frac{1}{\eta^2}\frac{\partial}{\partial\eta}\left(D_e\eta^2\frac{\partial C^*}{\partial\eta}\right) = \phi^2\frac{dX}{d\tau} \tag{3}$$

with boundary conditions

$$\frac{\partial C^*}{\partial\eta} = 0 \quad \text{at } \eta = 0$$
$$\frac{\partial C^*}{\partial\eta} = \frac{Sh(1-C^*)}{D_e^*} \quad \text{at } \eta = 1 \tag{4}$$

and the initial condition

$$X = 0 \text{ at } \tau = 0, \text{ for } 0 \le \eta \le 1 \tag{5}$$

The effective diffusivity was taken as varying with conversion according to

$$D_e^* = \frac{\epsilon^*\gamma(\epsilon_o)}{\gamma(\epsilon)} \tag{6}$$

and allowance was made for the change of porosity with reaction:

$$\epsilon^* = 1 - \frac{(Z-1)(1-\epsilon_o)X}{\epsilon_o} \tag{7}$$

Thus, in addition to the parameters S_o, ϵ_o, ϕ, β, Z, and Sh which are also required by the grain model, this model requires the parameter ψ. It was however shown (Bhatia and Perlmutter, 1980) that a value of the grain shape factor corresponding to the parameter ψ is implicitly assumed in the grain models.

In this paper the effects of pore size distribution are considered, and the random pore model is used to interpret data on the SO_2-lime reaction, particularly in terms of variation in pore structure. The broad interest in this reaction arises from its connection with environmental control, but its importance to the present purpose is to be found in the numerous reports of sensitivity to any treatment that affects pore structure. Harrington et al. (1968) reported considerable variation in reactivities of different limestones.

Marked differences in SO_2 absorption capacities were found in the pilot plant investigations of Attig and Sedor (1970), varying from 5 to 43 percent of theoretical. Falkenberry and Slack (1969), Potter (1969), and Borgwardt and Harvey (1972) have been successful in correlating such differences with the pore volume of the calcine. Hartman and Coughlin (1974, 1976) reacted limestones of different porosities and observed that the porosity is reduced as conversion proceeds, resulting in increased diffusional resistance in the particles, and in incomplete conversion of the solid. Ulerich et al. (1978) who adjusted the pore size distribution of calcines by varying the calcination atmosphere, also observed striking variations in sorption capacity.

Several investigators have previously applied the grain model to the study of the lime-SO_2 reaction. In their analysis Wen and Ishida (1973) treated the system as being governed by pore diffusion and chemical reaction, whereas Pigford and Sliger (1973) considered the reaction to be controlled by the diffusion of SO_2 through the pores and the accumulating product layer. In analyzing their data, Hartman and Coughlin (1976) used both a kinetic rate constant and a product layer diffusion coefficient. More recently Georgakis et al. (1979) applied a modified grain model, accounting also for the increase in grain size arising from the larger volume of $CaSO_4$ in comparison to CaO. Ramachandran and Smith (1977), and Chrostowski and Georgakis (1978) applied a single pore model to this reaction, neglecting however the intersections among reaction surfaces.

PORE-SIZE DISTRIBUTION

In general, the three parameters of the model (ϵ_o, S_o, and ψ) depend on the pore size distribution of the starting solid reactant. The initial porosity and surface (ϵ_o and S_o) can be obtained experimentally without recourse to any assumption of pore geometry, but the parameter ψ requires for its evaluation a third measure of the pore size distribution, namely L_o, for which there is no method of estimation that is free of some assumption about the pore structure.

In the present study the effect of various pore size distributions on the parameter ψ was investigated by considering the network of nonintersecting cylinders. Several well known unimodal distributions were considered and ψ was evaluated in terms of the appropriate normalized standard deviations. The pertinent equations (Bhatia and Perlmutter, 1980) are

$$L_{Eo} = \int_o^\infty f(r)dr \tag{8}$$

$$S_{Eo} = 2\pi\int_o^\infty rf(r)dr \tag{9}$$

$$V_{Eo} = -ln(1-\epsilon_o) = \pi\int_o^\infty r^2 f(r)dr \tag{10}$$

and

$$\psi = \frac{4\pi L_{Eo}}{S_{Eo}^2} \tag{11}$$

where $f(r)$ is the total nonoverlapped length of pores in the size interval $(r, r+dr)$. The results listed in Table 1 reveal that for unimodal distributions ψ is a function of only the porosity and normalized standard deviation, regardless of the assumed distribution. For a solid of given porosity, ψ becomes in effect a measure of the level of dispersion, taking on the value

$$\psi_u = -\frac{1}{ln(1-\epsilon_o)} \tag{12}$$

when the pores are of uniform size (i.e., $\sigma = 0$). It is also evident that the value of ψ increases with increasing σ for any of the distributions considered. Since Eq. 2 predicts that reaction rate also increases with ψ, a solid possessing pores of uniform size must offer the least intrinsic reactivity, for a given porosity and surface area.

Figure 1 shows the variation in structural parameter with standard deviation, both on normalized scales. Since $\sigma \le 1$ for the triangular and square distributions, the structural parameter can only rise to the limits of 1.17 and 1.33 respectively. For the normal distribution there is an initial rapid increase in ψ with increase in σ, but the ratio (ψ/ψ_u) asymptotically approaches $\pi/2$ for large σ values. The log-normal distribution allows the structural parameter to increase exponentially with σ^2 over the entire range $o < \sigma < \infty$.

TABLE 1. PORE STRUCTURE PARAMETER FOR SEVERAL PORE-SIZE DISTRIBUTIONS

Distribution Name	Distribution Function, $f(r)$	Pore Structure Parameter, ψ
Uniform	$L_{Eo}\delta(r-\mu)$	$\left[ln\left(\frac{1}{1-\epsilon_o}\right)\right]^{-1}$
Square	$\frac{L_{Eo}}{2\sigma\mu}\left[H(r-\mu+\sigma\mu)-H(r-\mu-\sigma\mu)\right]$	$\left[ln\left(\frac{1}{1-\epsilon_o}\right)\right]^{-1}\left[1+\frac{\sigma^2}{3}\right]$
Triangular	$0\ ;\ 0 \le r \le \mu(1-\sigma)$ $\frac{L_{Eo}}{\sigma^2\mu^2}\left[r+\sigma\mu-\mu\right]\ ;\ \mu(1-\sigma) \le r \le \mu$ $\frac{L_{Eo}}{\sigma^2\mu^2}\left[\mu+\sigma\mu-r\right]\ ;\ \mu \le r \le \mu(1+\sigma)$ $0\ ;\ \mu(1+\sigma) \le r$	$\left[ln\left(\frac{1}{1-\epsilon_o}\right)\right]^{-1}\left[1+\frac{\sigma^2}{6}\right]$
Log-normal	$\frac{L_{Eo}}{\sqrt{2\pi}r\sigma}\exp\left[-\frac{(lnr-ln\mu)^2}{2\sigma^2}\right]$	$\left[ln\left(\frac{1}{1-\epsilon_o}\right)\right]^{-1}[\exp(\sigma^2)]$
Normal	$\frac{2L_{Eo}\exp\left[-\frac{(r-\mu)^2}{2\sigma^2}\right]}{\sqrt{2\pi}\,\sigma\left[1+\mathrm{erf}\left(\frac{\mu}{\sqrt{2\sigma}}\right)\right]}H(0)$	$\left[ln\left(\frac{1}{1-\epsilon_o}\right)\right]^{-1}\left[\frac{G_1^2(\mu^2+\sigma^2)+\mu G_1 G_2}{(\mu G_1+G_2)^2}\right]$ where: $G_1 = 1 + erf(\mu/\sqrt{2}\,\sigma)$ $G_2 = \sqrt{\frac{2}{\pi}}\,\sigma\exp(-\mu^2/2\sigma^2)$

When the pore size distribution is bimodal, ψ would be expected to depend also on the frequencies of the modes. As the simplest example, the solid B may be considered to be comprised of pores of only two sizes: μ_1, and μ_2. Then Eqs. 8 to 10, and the definition of ψ, provide

$$\frac{\psi}{\psi_u} = \frac{\left[\frac{f_1}{\mu_1^2}+\frac{(1-f_1)}{\mu_2^2}\right]}{\left[\frac{f_1}{\mu_1}+\frac{(1-f_1)}{\mu_2}\right]^2} \tag{13}$$

where f_1 is the fraction of the porosity ϵ_o that is contributed by pores of size μ_1. It may be noted that $(\psi/\psi_u) > 1$ for all f_1 in the range $0 < f_1 < 1$, yielding a maximum at

$$f_1 = \frac{1}{1+(\mu_2/\mu_1)} \tag{14}$$

and demonstrating that there is an optimum distribution of the porosity between the two modes, since the solid is most reactive when ψ is largest. Similar optimal bimodal structures can be derived for any of the distributions of Table 1, suggesting a method of designing compacts made by pressing of microporous grains.

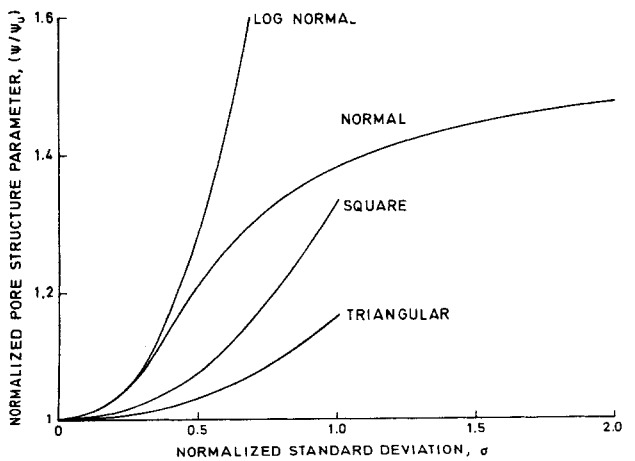

Figure 1. Effects of standard deviation of the pore size distribution on the pore structure parameter ψ for various distribution types.

MAXIMUM CONVERSION

If the solid product Q occupies a larger volume than did the consumed reactant B, a progressive decrease in porosity with conversion produces rapid attenuation in reaction rate and leads to cessation of reaction at incomplete conversion. In the absorption of SO_2 by limestone calcines in the presence of O_2, the $CaSO_4$ produced occupies about three times the volume of the CaO reacted. As expected Hartman and Coughlin (1974, 1976) reported incomplete conversions for this reaction, and analyzed the behaviour in terms of a spherical grain model. Using their random pore model Bhatia and Perlmutter (1981) also provided a quantitative description of this effect by considering the closure of surface pores and the loss of reaction resulting from the progressive inhibition of the transport of fluid A into the interior. When surface pore closure occurs the local conversion at the surface may be obtained by rearranging Eq. 7 to yield:

$$X_s = \frac{\epsilon_o}{(Z-1)(1-\epsilon_o)} \tag{15}$$

After this no further reaction is assumed to occur. Within the particles, however, the conversions will be lower after plugging of surface pores occurs, resulting in reduced overall maximum conversions.

To investigate the effect of pore structure on the maximum conversion, the reaction parameters were chosen to be similar to those of Hartman and Coughlin (1974), as listed in Table 2, but with $\psi = 2$, $S_o = 17.1 \times 10^6\ m^2/m^3$, and $D_p = 7.6 \times 10^{-13}\ m^2/s$. The reaction and concentration profiles in the solid particle are described by Eqs. 2 and 7. In addition, it was assumed that tortuosity is constant with reaction, i.e.:

$$D_e^* = \epsilon^* \tag{16}$$

with the initial value of D_e calculated from

$$D_{eo} = \frac{\epsilon_o}{\gamma} D_o \tag{17}$$

where

$$\gamma = 1/\epsilon_o \tag{18}$$

TABLE 2. MODEL PARAMETERS APPLIED TO DATA OF HARTMAN AND COUGHLIN (1974, 1976)

From Hartman and Coughlin (1976):

$a = b = 1$

$C_b = 3.2 \times 10^{-5}$ kmol/m^3

$Sh = \infty$

$\alpha_f = M/\rho = 16.9 \times 10^{-3}$ m^3/kmol

$\alpha_s = 52.2 \times 10^{-3}$ m^3/kmol

From the equations of Gavalas (1980) and the pore size distribution data in Hartman and Coughlin (1974):

$\epsilon_o = 0.52$

$$S_o = 2(1-\epsilon_o)\int_o^\infty \frac{d\nu}{r(1-\nu)} = 14.3 \times 10^6 \text{ m}^2/\text{m}^3$$

$$L_o = (1-\epsilon_o)\int_o^\infty \frac{d\nu}{\pi r^2(1-\nu)} = 8.48 \times 10^{13} \text{ m/m}^3$$

$\psi = 2.5$

From Figure 8

$k_s = 4.34 \times 10^{-5}$ m^4/kmol · s

From Model fit

$D_o = 8.6 \times 10^{-13}$ m^2/s

The initial diffusion coefficient D_o was obtained from

$$D_o = [D_A^{-1} + D_{Ko}^{-1}]^{-1} \tag{19}$$

with the initial Knudsen diffusion coefficient D_{Ko} expressed as:

$$D_{Ko} = 9700\left(\frac{2\epsilon_o}{S_o}\right)\sqrt{\frac{T}{M_A}} \tag{20}$$

A particle size diameter of 0.565 mm was used in accordance with the data of Hartman and Coughlin (1974). The solution procedure for these equations was the same as that employed in the prior development (Bhatia and Perlmutter, 1981).

The results summarized in Figure 2 were obtained by allowing the porosity and surface area to vary from the reference values given above, showing that maximum conversion drops markedly as initial surface is increased, but improves sharply with porosity. Evidently the smaller pores associated with large surface serve to significantly restrict flow of reactant into the particle interior, whereas large porosity corresponds to large mean pore size and allows greater conversion by delaying pore plugging.

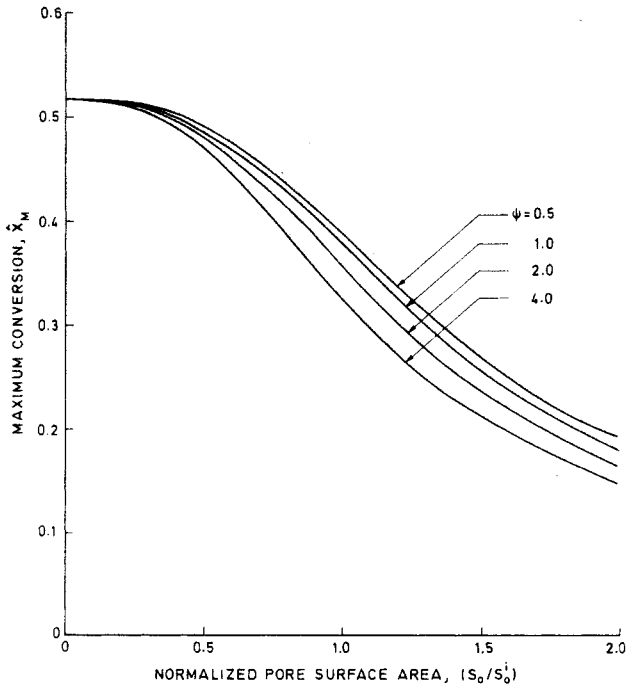

Figure 3. Effect of pore surface area on maximum conversion for various values of the pore structure parameter.

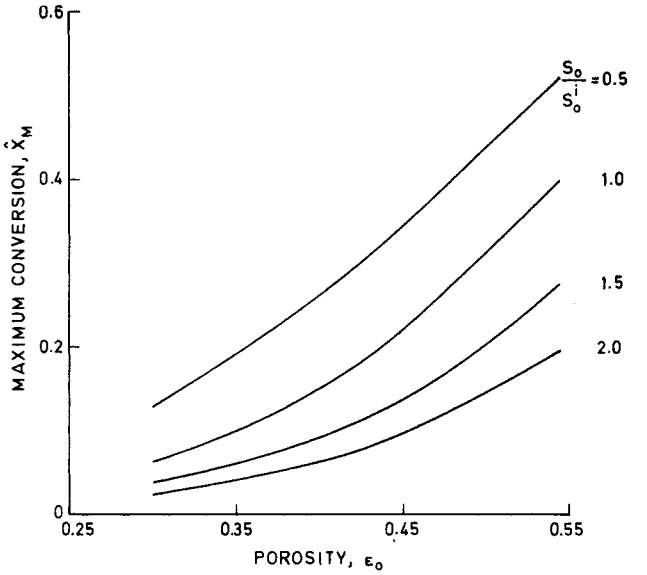

Figure 2. Effect of porosity on maximum conversion for various values of surface area.

In comparison, the effect of the pore structure parameter ψ on the maximum conversion is less pronounced, as shown in Figure 3, indicating that the behavior is less dependent on the specific distribution shape than it is on surface and porosity. There is, however, a small decrease in ultimate conversion with increase in ψ. Practical design must therefore strike a balance between improved utilization of solid on the one hand, and greater reactivity and smaller residence times on the other. The former advantage stems from less dispersed pore structures (small ψ) and small surface area, the latter from greater dispersion (large ψ), and large surface area.

CONVERSION—TIME BEHAVIOR

Selected solutions to Eqs. 2 to 7 are shown in Figure 4, indicating as before that the dispersion in pore sizes does not strongly affect the reaction, in contrast to the result previously given (Bhatia and Perlmutter, 1980) for the kinetic regime. The difference may be attributed to the strong product layer diffusional resistance which inhibits the reaction rate. This leads to the observation that while the grain shape factor varies with ψ, any inaccuracies arising from arbitrary choice of grain shape are likely to be obscured by the large product layer diffusional resistance.

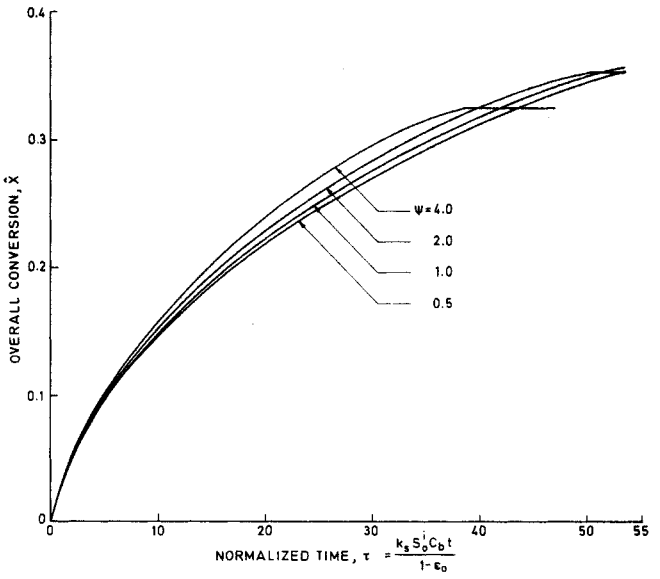

Figure 4. Effect of the pore structure parameter on conversion-time behavior.

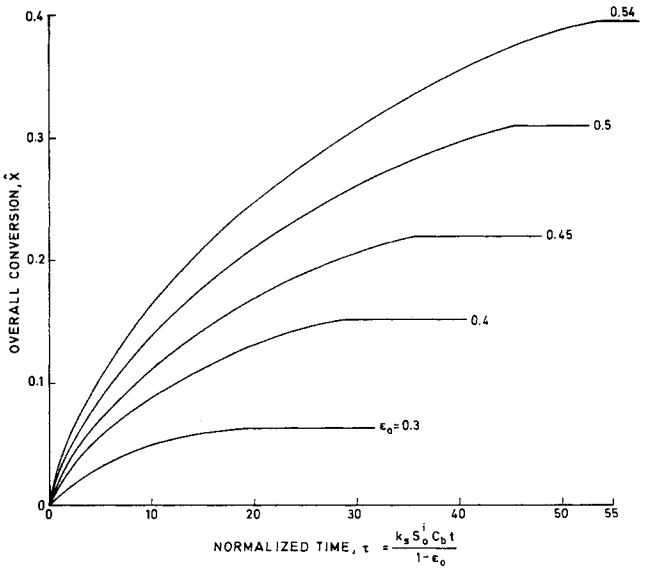

Figure 5. Effect of porosity on conversion-time behavior.

TABLE 3. MODEL PARAMETERS APPLIED TO DATA OF BORGWARDT (1970)

From Borgwardt (1970), and Borgwardt and Harvey (1972)

a	$= b = 1$
C_b	= calculated at each temperature for 3000 ppm SO_2 (dry basis)
Sh	$= \infty$
α_l	$= 16.9 \times 10^{-3}$ m³/kmol
α_s	$= 52.2 \times 10^{-3}$ m³/kmol
ω_0	$= 0.54$
ρ_b	$= 1.59 \times 10^3$ kg/m³
R_0	$= 48\ \mu$m
ϵ_0	$= 0.56$ } from porosimetry data given in reference for calcine #9.
S_0	$= 5.9 \times 10^6$ m²/m³ }
ψ	= 1.2 (calculated assuming a uniform pore size)

Figure 3 shows the enhanced reaction rates and ultimate conversions achieved with increases in porosity, mostly by the reduced pore diffusional resistance, and partly via the reduced product layer diffusional resistance. This behavior is consistent with the experimental findings of Potter (1969) that CaO utilization correlated well with the pore volume of the calcine.

With increase in the surface area several opposing effects occur. The pore diffusional resistance increases, while the product layer diffusional resistance decreases (because $\beta \propto 1/S_0$). In addition, the larger available reaction surface enhances overall rate. Figure 6 shows that the larger reaction rate from the availability of greater surface initially dominates these effects when the surface area is changed, and as a result the conversion process is accelerated. After $(S_0/S_0^i) > 0.9$ is reached, however, only marginal improvement in rate occurs because of the enhanced pore diffusional resistance. The ultimate overall conversion continues to fall rapidly as surface pore closure reduces the rate of transport of fluid A into the interior.

TABLE 4. RATE PARAMETERS ESTIMATED FROM DATA OF BORGWARDT (1970)

T, °C	Estimated from Initial Rates $k_s \times 10^5$ (m⁴/kmol · s)	Estimated from Conversion-Time Data β	Calculated from estimated value of β $D_e \times 10^{12}$ (m²/s)
650	1.2	50	1.25
760	2.55	22	6.04
870	4.74	13	19
980	8.34	6.3	69

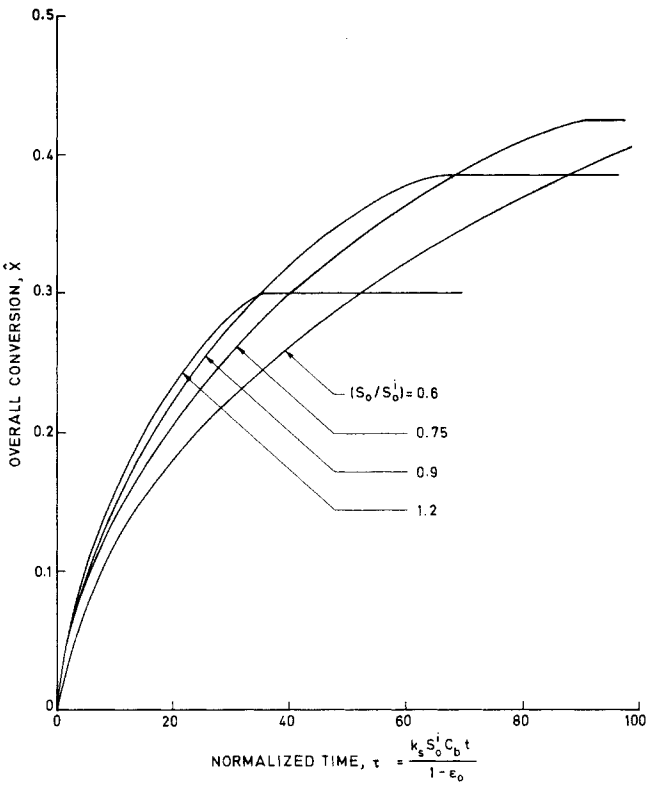

Figure 6. Effect of pore surface on conversion-time behavior.

APPLICATION TO THE SO_2—LIME REACTION

In order to demonstrate the application of the pore structure arguments in conjunction with the random pore model, a detailed analysis was undertaken of the data of Borgwardt (1970) on the lime-SO_2 reaction at various temperatures in the range of 923 to 1253 K and of the data of Hartman and Coughlin (1974, 1976) for the same reaction at 1123 K for three different particle sizes. A straightforward computation of k_s at each temperature was obtained from the initial rate data of Borgwardt (1970), on reacting particles of 98 micron diameter, by solving Eqs. 2 to 5 to yield:

$$\left(\frac{dX}{dt}\right)_{t=0} = \frac{3k_s S_0 C_b}{\phi(1-\epsilon_0)}\left[\frac{1}{\tanh(\phi)} - \frac{1}{\phi}\right] \qquad (21)$$

where the effect of bulk flow, neglected in Eq. 3, should be insignificant because the reactant gas is dilute. Since ϕ is a function of k_s, an iterative procedure was used to obtain k_s from Eq. 21 and the initial rates of Borgwardt (1970). In the calculation, D_{e0} was evaluated from Eqs. 17 to 20, and the other parameters used are contained in Table 3. The results are listed in Table 4 and presented on the usual Arrhenius coordinates in Figure 7, yielding an activation energy of 56.4 MJ/kmol.

In evaluating these findings it should be noted that several conflicting values of the rate constant for this reaction have appeared in the literature. Hartman and Coughlin (1976) obtained $k_s = 111.5 \times 10^{-5}$m⁴/kmol · s at 1123 K from their data analyzed at 4% conversion. From the same data, but using an initial rate analysis, Ramachandran and Smith (1977) calculated k_s to be 1.72×10^{-5}m⁴/kmol · s at 1123 K. Wen and Ishida (1973) found $k_s = 0.9 \times 10^{-5}$m⁴/kmol · s at 1123 K by averaging data of several prior investigations. The data of Borgwardt and Harvey (1972) indicate that considerable variation may be found among calcines obtained from different limestones.

Simultaneous solution of Eqs. 2 to 7 and 16 to 20 can provide predictions of conversion-time dependence for specific choices of the various parameters. To test such predictions against the data of Borgwardt (1970), the system constants listed in Table 3 were used leaving only the single variable β as a fitting param-

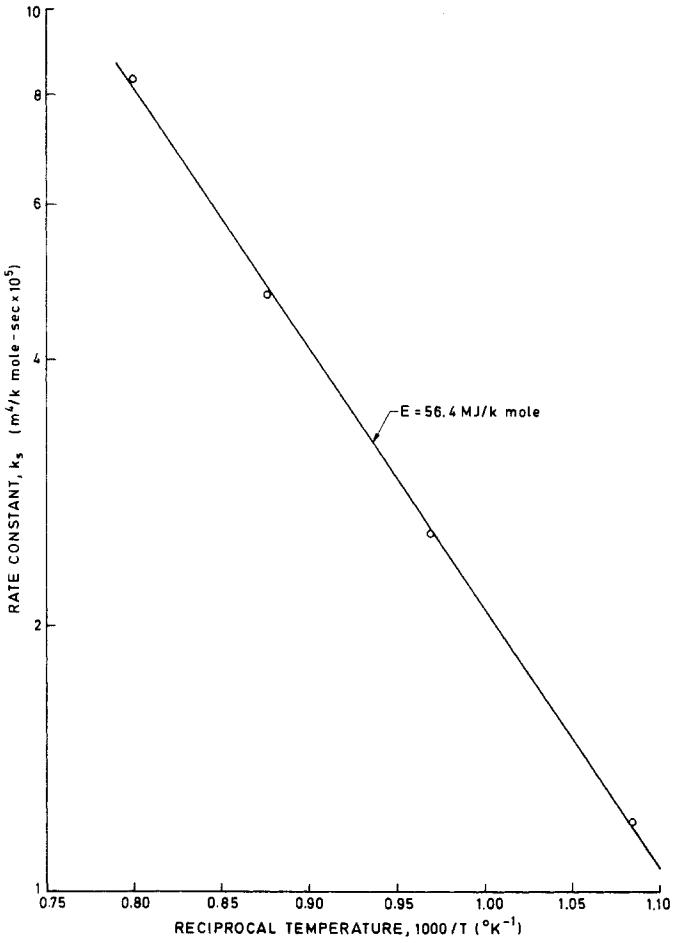

Figure 7. Arrhenius plot for reaction rate constant k_s.

eter at each temperature. The parameter Z in Table 3 was estimated for the limestone of Borgwardt using the relation

$$Z = 1 + \frac{\rho\alpha_l(\alpha_s/\alpha_l - 1)}{M} \tag{22}$$

with

$$\rho = \frac{\rho_b\omega_o}{(1 - \epsilon_o)} \tag{23}$$

Figure 8 superimposes the computed results on the experimental data in the reference. The best fit values of β are listed in Table 4 along with the corresponding values of D_μ calculated from them. The Arrhenius plot in Figure 9 shows that the diffusion through the product layer occurs via an activated mechanism, requiring an energy of 120 MJ/kmol.

Hartman and Coughlin (1974, 1976) also provided rate data for the same reaction at 1123 K for each of three different particle diameters: 0.565, 0.9 and 1.13 mm. Table 2 has already summarized the values of the parameters applicable to their data. As with the Borgwardt data, the value of β was parametrically varied to find the best fit. Figure 10 shows the agreement between the calculated conversion-time curves and the experimental data at the best fit value of $\beta = 200$. The value of D_μ corresponding to this level of β is 8.6×10^{-13} m^2/s. Hartman and Coughlin (1976) obtained the value of D_μ to be 6×10^{-13} m^2/s by using their spherical grain model. The same authors also provided experimental data for a particle size of 0.565 mm on the effect of SO_2 concentration on the conversion achieved after exposure times 300 and 1080 s; these measurements are consolidated in Figure 11 using only the single group $(C_b t)$ as an independent variable. The model predictions are shown as the solid line in Figure 11.

Additional computations showed that the conversion-time curves of Figure 10 are not sensitive to the choice of k_s over the

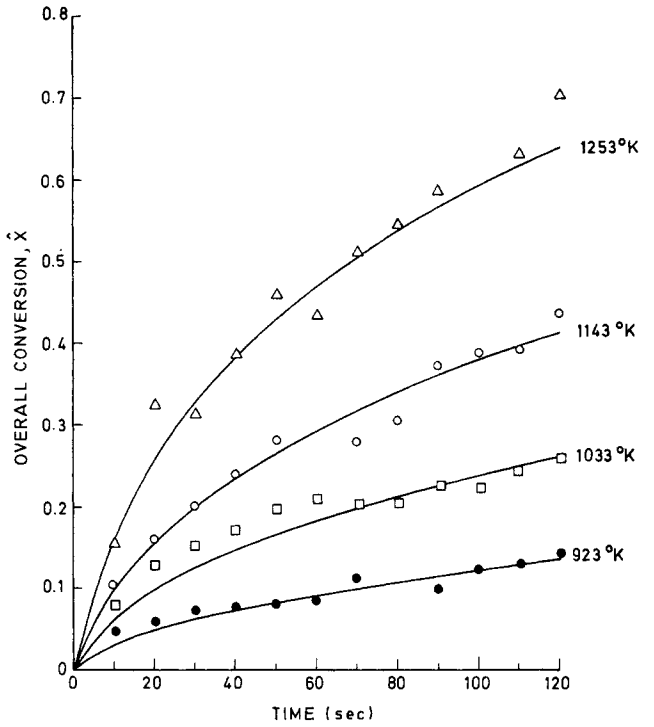

Figure 8. Application of random pore model to data of Borgwardt (1970). Solid lines represent model calculations.

range of values reported by the previous investigators. This finding indicates that the reaction is strongly controlled by product layer diffusion under the conditions of Hartman and Coughlin (1976), in agreement with their own observations using the grain model. This observation is also consistent with the analysis of Pigford and Sliger (1973) who, in their treatment of the limestone sulfation data of Coutant (1970), and of calcine #4 of Borgwardt (1970), assumed that the reaction was controlled by the two participating diffusional processes. Further support for this observation may be obtained by noting that for large values of β such as that estimated for the data of Hartman and Coughlin:

$$[\beta Z(\sqrt{1 - \psi ln\,(1 - X)} - 1)/\psi] >> 1$$

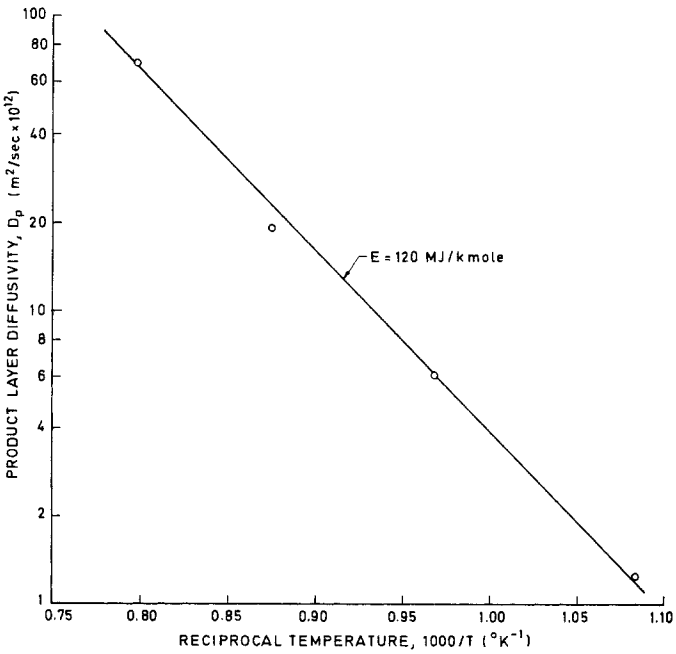

Figure 9. Temperature dependence of the product layer diffusivity estimated from data of Borgwardt (1970).

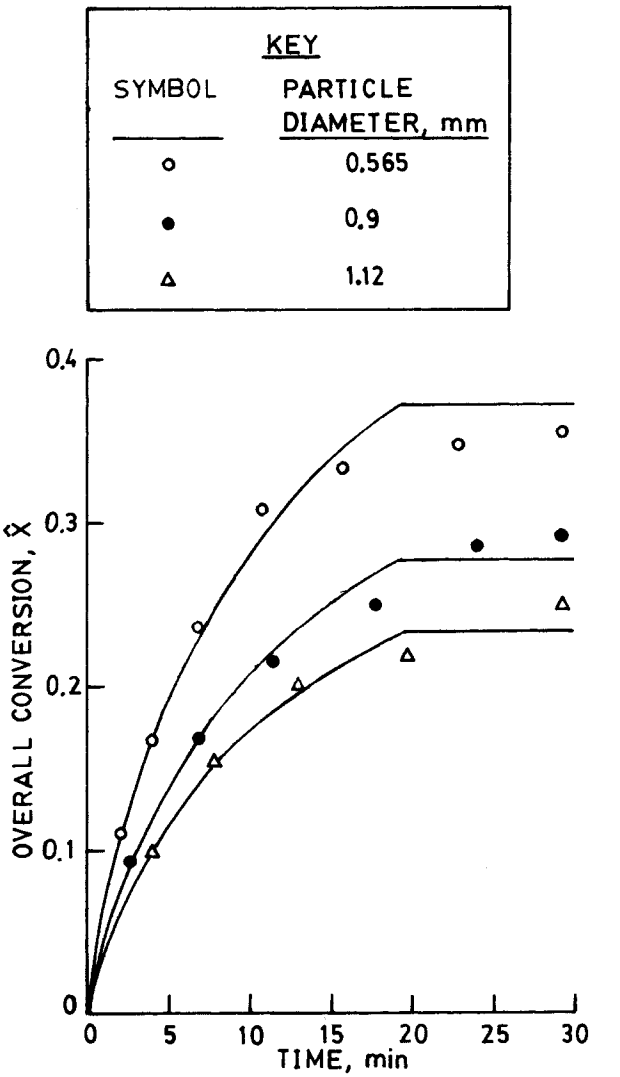

Figure 10. Application of Random Pore Model to data of Hartman and Coughlin (1976). Solid lines represent model calculations.

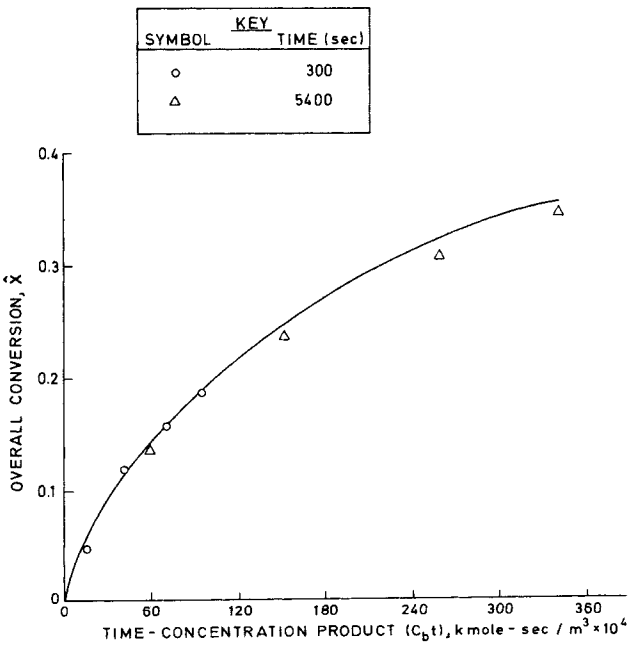

Figure 11. Generalized conversion-time plot using ($C_b t$) as an independent variable. Solid curve represents model predictions; circles and triangles represent experimental points of Hartman and Coughlin (1976).

except for very small conversions. Consequently, Eq. 2 may for all practical purposes be rewritten in dimensional form as:

$$\frac{dX}{dt} = \left[\frac{S_o^2 M b D_p C_b}{2Z(1-\epsilon_o)^2 a\rho}\right] \frac{C^*(1-X)\sqrt{1-\psi \ln(1-X)}}{(\sqrt{1-\psi \ln(1-X)}-1)} \quad (24)$$

which is the result for diffusion control, independent of the rate constant. This accounts for the small difference in the estimated values of D_p, inspite of the large difference in the values of the rate constant used, between this analysis and that of Hartman and Coughlin (1976).

This model predicts that as a result of rapid surface pore closure, reaction will cease at about 20 minutes for each particle size, under the conditions of the Figure 10 data. In fact, although the added conversion is very small, Hartman and Coughlin (1976) observed the reaction to continue for a longer time, but at a considerably slower rate. Also, their microscopic examinations revealed that the surface porosity never disappeared entirely, but attained a small residual value allowing some diffusion to continue. Hartman and Coughlin were able to fit the data over the full 3600-s time span by using the limiting porosity as an added fitting parameter in their grain model. Such a fit could be performed with the present model as well, if the added parameter were used.

DISCUSSION

Reaction Mechanism

By fitting the model to the experimental data of Borgwardt (1970), and of Hartman and Coughlin (1974, 1976) estimates were obtained of the product layer diffusivity for the calcines used by these investigators. The results are in the range often found for diffusion in the solid state and show an Arrhenius temperature dependence that might be expected for solid state diffusion. In addition the activation energy for this diffusion is in the range of magnitudes often found for ionic motion in solids. This suggests the participation of solid state processes in this reaction. Such a view would be consistent with the fact that the crystal molar volume of $CaSO_4$ is three times that of CaO, so that a non-porous protective layer would be expected to form on the CaO surface soon after the start of the reaction preventing further contact of CaO with the reacting gas.

Further reaction may then involve the chemisorption of SO_2 and oxygen in the form of charged complexes on the $CaSO_4$ surface, and motion of ions in this nonporous layer. Ionic reactions may then occur at the gas solid and solid-solid interfaces. The precise nature of the moving species cannot be determined from kinetic data alone, but would require other measurements pertaining to the conduction properties of $CaSO_4$, and its defect structure.

The net result of these solid state processes is a parabolic rate with the associated effective product layer diffusivity. Evidence for such processes has been reported for reactions involving the oxidation of metals when the oxide forms a non-porous protective layer over the metal (Hauffe, 1976). This interpretation notwithstanding, it should be noted that several other plausible mechanisms might also be consistent with the data. As an example it might indeed be that gaseous SO_2 and O_2 diffuse through sub-microscopic cracks in the deposited layer of $CaSO_4$. If crack nucleation in the $CaSO_4$ occurred by an activated process it could result in the temperature-dependent behavior of D_p found in this analysis.

Bimodal Distributions

The calcine of Hartman and Coughlin (1974, 1976) offers an interesting example of a bimodal pore size distribution. If their pore-size distribution which possessed maxima at 290 Å and

10,000 Å is approximated by a discrete distribution having pores of only two sizes, Eq. 14 calls for an optimal choice at:

$$f_1 = \frac{1}{1 + (10000/290)} = 0.028$$

and correspondingly Eq. 13 provides a maximum value of $(\psi/\psi_u) = 9.13$. In fact each mode contributed about half the total porosity to the calcine tested giving $(\psi/\psi_u) = 1.89$. This result may be compared with $(\psi\psi_u) = 1.84$, obtained by the prior calculation (Table 2) which used the continuous distribution reported by Hartman and Coughlin (1974). The discrete two-size approximation differs only negligibly from the continuous result. This agreement notwithstanding, it should be noted that the particular distribution reported is quite removed from one that would be optimal in producing a structure for maximum intrinsic reactivity. Modified calcining conditions may be expected to result in the more desirable structure.

Optimal Pore Structure

Consideration of Figure 6 shows that the largest surface that can produce a given conversion is also the surface area that corresponds to minimum time. Figures 2 and 3 can therefore provide the optimal surface and parameters ϵ_o and ψ of the pore structure that will achieve the chosen conversion level. Since the pore structure area and porosity of solids can often be adjusted by sintering, the above analysis should indicate suitable criteria for selecting conditions for such a pretreatment. This is especially true for limestones since the pore volume distributions of their calcines are strongly dependent on the calcining atmosphere and temperature (Ulerich et al., 1978; McClellan and Eades, 1970; Mullins and Hatfield, 1970).

ACKNOWLEDGMENT

This research was initially funded by the U.S. Department of Energy, Office of Basic Energy Science under Contract No. EY-76-S-02-2747, and completed under National Science Foundation support.

NOMENCLATURE

a,b = stoichiometric coefficients
C = local concentration of fluid A
C_b = bulk concentration of fluid A
C^* = C/C_b
D_o = initial diffusion coefficient of A
D_A = molecular diffusivity of A
D_e = effective diffusivity of fluid A in particle
D_{eo} = initial value of D_e
D_e^* = D_e/D_{eo}
D_{Ko} = initial Knudsen diffusivity of A
D_p = effective diffusivity of fluid A in product layer
E = activation energy
f_1 = fraction of total porosity contributed by pores of radius μ_1
$H(r)$ = heavyside operator: 0 for $r < 0$; 1 for $r \geq 0$
k_m = boundary layer mass transfer coefficient
k_s = rate constant for surface reaction
$l(r)$ = pore length distribution function
L_o = total length of pore system per unit volume, at $t = 0$
L_{Eo} = initial total length of nonoverlapped cylindrical system
M = molecular weight of solid B
M_A = molecular weight of fluid A
p, q = stoichiometric coefficients
r = pore radius
R = radial position
R_o = particle radius
S_o = initial pore surface area per unit volume
S_o' = reference value of S_o
S_{Eo} = initial total surface area of nonoverlapped cylindrical system
Sh = $k_m R_o/D_{eo}$, Sherwood Number
t = time
t_s = pore closure time
T = temperature
X = local conversion
$\hat{X}$ = overall conversion = $3\int_0^1 X\eta^2 d\eta$
$\hat{X}_m$ = maximum overall conversion
X_s = local conversion at surface upon pore closure
Z = ratio of volume of solid phase after reaction to that before reaction

Greek Letters

α_l = molar volume of CaO
α_s = molar volume of $CaSO_4$
β = $\dfrac{2k_s a\rho(1-\epsilon_o)}{MbD_p S_o}$
ϵ = porosity
ϵ_o = ϵ at $t = 0$
ϵ^* = ϵ/ϵ_o
$\gamma(\epsilon)$ = tortuosity
μ = pore radius
μ_1, μ_2 = pore radii for bimodal distribution
η = R/R_o
ω_o = mass fraction of reactant B in initial solid particles
ϕ = $R_o\sqrt{\dfrac{k_s a\rho S_o}{MbD_{eo}}}$, Thiele Modulus
ψ = $\dfrac{4\pi L_o(1-\epsilon_o)}{S_o^2}$, structural parameter
ψ_u = value of ψ for a uniform pore-size distribution, defined in Eq. 11
ρ = mass of solid B per unit volume of solid phase
ρ_b = initial bulk density of solid
σ = normalized standard deviation
τ = $k_s C_b S_o t/(1-\epsilon_o)$, dimensionless time
τ_s = pore closure time = $k_s C_b S_o t_s/(1-\epsilon_o)$

LITERATURE CITED

Attig, R., and C. Sedor, "Additive Injection for Sulfur Dioxide Control," Babcock & Wilcox Co., Research Center Report 5460 (1970).

Bhatia, S. K., and D. D. Perlmutter, "A Random Pore Model for Fluid-Solid Reactions: I. Isothermal, Kinetic Control," *AIChE J.*, **26**, 379 (1980).

Bhatia, S. K., and D. D. Perlmutter, "A Random Pore Model for Fluid-Solid Reactions: II. Diffusion and Transport Effects," *AIChE J.* (March, 1981).

Borgwardt, R. H., "Kinetics of the Reaction of SO_2 with Calcined Limestone," *Environ. Sci. Technol.*, **4**, 59 (1970).

Borgwardt, R. H., and R. D. Harvey, "Properties of Carbonate Rocks Related to SO_2 Reactivity," *Environ. Sci. Technol.*, **6**, 350 (1972).

Chrostowski, J. W., and C. Georgakis, "Pore Plugging Model for Gas-Solid Reactions," Fifth International Symposium on Chemical Reaction Engineering, Houston, TX (1978).

Coutant, R. W., R. Simon, B. Campbell, and R. E. Barrett, "Investigations of the Reactivity of Limestone and Dolomite for Capturing SO_2 from Flue Gas," Battelle Memorial Institute, Columbus, OH (1970).

Falkenberry, H. L., and A. V. Slack, "SO_2 Removal by Limestone Injection," *Chem. Eng. Prog.*, **65**, 61 (1969).

Georgakis, C., C. W. Chang, and J. Szekely, "A Changing Grain Size Model for Gas-solid Reactions," *Chem. Eng. Sci.*, **34**, 1072 (1979).

Harrington, R. E., R. H. Borgwardt, and A. E. Potter, "Reactivity of Selected Limestones and Dolomites with Sulfur Dioxide," *Amer. Ind. Hyg. Assoc. J.*, **29**, 152 (1968).

Hartman, M., and R. W. Coughlin, "Reaction of Sulfur Dioxide with Limestone and the Influence of Pore Structure," *Ind. Eng. Chem. Proc. Des. Dev.*, 13, 248 (1974).
Hartman, M., and R. W. Coughlin, "Reaction of Sulfur Dioxide with Limestone and the Grain Model," *AIChE J.*, 22, 490 (1976).
Hauffe, K., "Gas-solid Reactions—Oxidation," in Treatise on Solid State Chemistry, 4, 389, N. B. Hannay, ed., Plenum Press, New York (1976).
McClellan, G. H., and J. L. Eades, "The Textural Evolution of Limestone Calcines," *The Reaction Parameters of Lime*, ASTM Special Tech. Pub. 472, 209 (1970).
Mullins, R. C., and J. D. Hatfield, "Effects of Calcination Conditions on the Properties of Lime," *The Reaction Parameters of Lime*, ASTM Special Tech. Pub. 472, 117 (1970).
Potter, A. E., "Sulfur Oxide Capacity of Limestones," *Am. Ceram. Soc. Bull.*, 48, 855 (1969).
Pigford, R. L., and G. Sliger, "Rate of Diffusion Controlled Reaction between a Gas and a Porous Solid Sphere," *Ind. Eng. Chem. Proc. Des. Dev.*, 12, 85 (1973).
Ramachandran, P. A., and J. M. Smith, "A Single-Pore Model for Gas-Solid Non-Catalytic Reactions," *AIChE J.*, 23, 353 (1977).
Szekely, J., J. W. Evans, and H. Y Sohn, *Gas-Solid Reactions*, Academic Press, London (1976).
Ulerich, N. H., E. P. O'Neill, and D. L. Keairns, "A Thermogravimetric Study of the Effect of Pore Volume—Pore Size Distribution on the Sulfation of Calcined Limestone," *Thermochimica Acta*, 26, 269 (1978).
Wen, C. Y., and M. Ishida, "Reaction of Sulfur Dioxide with Particles Containing Calcium Oxide," *Environ. Sci. Technol.*, 7, 703 (1973).

Manuscript received February 29, 1980; revision received July 14, and accepted July 16, 1980.

Wrong-Way Behavior of Packed-Bed Reactors:

1. The Pseudo-Homogeneous Model

P. S. MEHTA
W. N. SAMS
and
D. LUSS

Department of Chemical Engineering
University of Houston
Houston, Texas 77004

A sudden reduction in the feed temperature to a packed-bed reactor leads to a transient temperature rise, which is referred to as the wrong-way behavior. A pseudo-homogeneous plug-flow model is used to analyze the structure of this transient behavior. The key parameters which determine the magnitude of this response are the dimensionless adiabatic temperature rise, activation energy, heat transfer capacity, coolant temperature, magnitude of temperature drop and length of the reactor. A simple expression is derived for predicing the maximum transient temperature rise.

SCOPE

When the temperature of the feed to a packed-bed reactor is suddenly decreased a transient temperature rise may occur. This surprising dynamic feature is caused by the difference in the speed of propagation of the concentration and temperature disturbances and is referred to as the wrong-way behavior. This response was predicted originally by Boreskov and Slinko (1965) and Crider and Foss (1966), and was observed by many investigators (Hoiberg et al., 1971; Van Doesberg and DeJong, 1976a, 1976b; Hansen and Jorgensen, 1977; Sharma and Hughes, 1979).

The wrong-way behavior may damage the catalyst and initiate undesired side reactions. The need to avoid it complicates the control policies and start-up and shut-down procedures of packed-bed reactors. At present lengthy numerical simulations are required to determine when this behavior may be encountered and its magnitude.

The purpose of this work is to identify the key rate processes and parameters which cause this behavior and to develop a simple technique for a priori prediction of the highest transient temperature without solving the transient equations. This is accomplished by analyzing the dynamic response of a plug-flow pseudo-homogeneous model of a packed-bed reactor using the method of characteristics. First, we determine the structure of the solution and the conditions for which a wrong-way behavior occurs for a zeroth-order reaction in either a cooled or an adiabatic reactor. We examine then how this behavior is modified by a rate expression for which the reactants are not completely consumed and by intraparticle diffusional resistances.

CONCLUSIONS AND SIGNIFICANCE

The analysis indicates that for a zeroth-order reaction the wrong-way behavior occurs only if the reactor is longer than a critical length of z_{ci}. The highest transient temperature increases with reactor length until the reactor is of length z_{cn}. For any reactor shorter than z_{cn} and longer than z_{ci} the highest transient temperature is encountered at the exit of the reactor. For a cooled reactor longer than z_{cn} the limiting transient-peak temperature occurs at z_{cn}. For an adiabatic reactor the limiting transient-peak temperature is encountered at all points downstream of z_{cn}.

0001-1541-81-4378-0234-$2.00. © The American Institute of Chemical Engineers, 1981.